JOURNAL OF THERMOPHYSICS AND HEAT TRANSFER
Vol. 19, No. 3, July–September 2005

# Partially Coherent Spectral Transmittance of Dielectric Thin Films with Rough Surfaces

B. J. Lee,* V. P. Khuu,† and Z. M. Zhang‡
*Georgia Institute of Technology, Atlanta, Georgia 30332*

**The effects of scattering and partial coherence on the transmittance of thin films with rough surfaces are investigated. For the rough side, the rms roughness is between 0.3 and 0.7 $\mu$m, whereas the autocorrelation length ranges from 1 to 36 $\mu$m. Scalar scattering theory (SST) is used to account for the scattering losses in the specular direction due to surface roughness, and then the calculated transmittance is spectrally averaged over the coherence spectral width. The spectral averaging method takes into consideration the effect of partial coherence. A Fourier-transform infrared spectrometer measures the near-normal transmittance in the midinfrared region from 2- to 20-$\mu$m wavelengths. Comparison of the calculated transmittance with that of the measured transmittance shows that the combination of SST with spectral averaging can correctly predict the measured fringe contrast and fringe flipping, whereas SST alone does not result in quantitative agreement with the experiments. A coherence function is introduced to characterize the degree of coherence as a function of wave number for samples with or without a rough surface. Furthermore, it is shown that SST is not applicable to surfaces whose autocorrelation length is greater than the wavelength of the incident radiation.**

## Nomenclature

| | | |
|---|---|---|
| $d$ | = | thickness, m |
| $i$ | = | $\sqrt{-1}$ |
| $k$ | = | imaginary part of the complex refractive index |
| $n$ | = | real part of the complex refractive index |
| $R$ | = | reflectance |
| $r$ | = | Fresnel reflection coefficient |
| $S$ | = | scattering factor |
| $T$ | = | transmittance |
| $\bar{T}$ | = | spectrally averaged transmittance |
| $t$ | = | Fresnel transmission coefficient |
| $\beta$ | = | phase shift, rad |
| $\Delta\nu$ | = | free spectral range, $m^{-1}$ |
| $\delta\nu$ | = | coherence spectral width, $m^{-1}$ |
| $\theta$ | = | polar angle, rad |
| $\lambda$ | = | wavelength of the incident radiation in vacuum, m |
| $\nu$ | = | wave number, $m^{-1}$ |
| $\sigma$ | = | rms roughness, m |
| $\tau$ | = | internal transmissivity |
| $\Phi$ | = | fringe contrast |
| $\phi$ | = | coherence function |

*Subscripts*

| | | |
|---|---|---|
| coh | = | coherent |
| $p$ | = | $p$ polarization |
| $r$ | = | reflection |
| $s$ | = | $s$ polarization |
| $t$ | = | transmission |

Presented as Paper 2004-2466 at the AIAA 37th Thermophysics Conference, Portland, OR, 28 June–1 July 2004; received 28 July 2004; revision received 12 November 2004; accepted for publication 12 November 2004. 

*Graduate Research Assistant, George W. Woodruff School of Mechanical Engineering.

†Graduate Research Assistant; currently Mechanical Engineer, Northrop Grumman Corporation, Electronic Systems, Baltimore, MD 21203.

‡Associate Professor, George W. Woodruff School of Mechanical Engineering. Associate Fellow AIAA.

## Introduction

A THOROUGH understanding of the radiative properties of thin films is important for the development of reliable models in many industrial applications, such as optoelectronics and semiconductor processing. Accurate prediction of the spectral transmittance becomes challenging when complexity arises from light scattering by rough surfaces. Scalar scattering theory (SST), which uses modified Fresnel coefficients to account for the losses of the energy in the specularly reflected or transmitted beams, has been applied in a number of studies since the 1960s (Refs. 1–7). Filinski[2] investigated the effects of surface roughness and optical inhomogeneity on the radiative properties of thin films based on SST. Several studies extended SST to the case of multilayer structures using the matrix formulation.[3–5] In modeling the radiative properties of chemical vapor deposited (CVD) diamond, Robins et al.[6] applied SST to include surface scattering and determined optical constants of CVD diamond by comparison with the measurements in the visible and near-ultraviolet spectral regions. More recently, Poruba et al.[7] studied the origins of enhanced light absorption in solar cells and used SST to model the influence of light scattering on the absorptance. They considered both surface and bulk scattering and extracted the absorption coefficient from the measured transmittance and reflectance spectra.

When the effect of partial coherence is significant, SST alone cannot accurately predict the transmittance of thin films. Partial coherence theory considers the intermediate regime between the coherent limit (wave optics) and incoherent limit (geometric optics). In reality, partial coherence is often caused by the limited resolution of the instrument, beam divergence, as well as nonparallelism and surface roughness of the sample. Wong et al.[8] attributed the reflectance peaks of multilayer structure to the cross correlation of the phase functions among layers. Chen and Tien[9] predicted the radiative properties of a thin film using the partial coherence theory and developed a regime map to help determine when wave optics or geometric optics may be applied. Richter et al.[10] extended the partial coherence formulation to multilayer structures and verified it with experiments. Zhang[11] used the partial coherence theory to express the radiative properties of a thin film with coatings in the form of a superposition and compared the calculated results to the measurements with a Fourier-transform infrared (FT–IR) spectrometer. Furthermore, Anderson and Bayazitoglu[12] compared directional and hemispherical radiative properties calculated from wave optics, geometric optics, and partial coherence formulation and, subsequently, developed regime maps for different incidence

conditions. Grossman and McDonald[13] studied the wave number dependence of the degree of coherence on the transmittance of a polished silicon wafer in the far infrared.

Even though many studies showed that SST could yield reasonable agreement with certain experiments, few studies simultaneously considered partial coherence. Petrich and Stenzel[14] considered the coherence disturbance of light incident on rough surfaces by integrating the transmission coefficients over a Gaussian distribution of the film thickness. To model the transmittance of thin films with rough surfaces considering partial coherence, the present study combines SST with the spectral averaging method, which has been proven to produce the same results as those predicted by the partial coherence formulation.[9–11] A coherence function is introduced to characterize the degree of coherence as a function of wave number. An FT–IR spectrometer is used to measure the transmittance of several double-side-polished (DSP) and single-side-polished (SSP) films in the midinfrared spectral range. The measured spectra are compared with the calculated results to demonstrate the applicability of the method. An atomic force microscope (AFM), a surface profilometer, and an optical microscope provide topographic data for further validation of the model.

## Scalar Scattering Theory

Figure 1 shows the transmittance and reflectance of a thin film with rough surfaces. A dielectric layer of average thickness $d$ with internal absorption but no internal scattering is placed in the ambient air. In the present study, the optical property of air is assumed to be the same as that of vacuum. The transmission coefficient of a thin film (medium 2) can be calculated from Airy's formula, namely, (see Ref. 15),

$$t = \frac{t_{12}t_{23}\sqrt{\tau}e^{i\beta}}{1 - r_{21}r_{23}\tau e^{i2\beta}} \tag{1}$$

where $r_{21}$ and $r_{23}$ are the Fresnel reflection coefficients, $t_{12}$ and $t_{23}$ are the Fresnel transmission coefficients, $\beta$ is the phase shift of the electric field on traversing the film, and $\tau$ is the internal transmissivity of the film. Notice that these parameters are generally complex quantities that depend on the complex refractive index of the film material. When the extinction coefficient $k_2$ is much smaller than the refractive index $n_2$, as is often the case for a dielectric, the phase shift is given by

$$\beta = (2\pi n_2/\lambda)d\cos\theta_2$$

the internal transmissivity is

$$\tau = \exp\left(-\frac{4\pi k_2 d}{\lambda\cos\theta_2}\right)$$

and $k_2$ can be neglected in calculating the Fresnel coefficients (see Ref. 16). Here, $d$ is the film thickness and $\theta_2 = \sin^{-1}(n_1\sin\theta_1/n_2)$, given by Snell's law. Because the first and third media are identical (air), the spectral transmittance can be calculated for each polarization using the following equation:

$$T = tt^* \tag{2}$$

where the asterisk denotes the complex conjugate. When the incident radiation is unpolarized, the transmittance is averaged over the two polarizations, which are the same at normal incidence.

To model the losses in the reflected or transmitted energy in the specular direction due to scattering, the Fresnel coefficients are modified by the scattering factors that depend on the rms roughness. The derivation of the scattering factor is based on the assumptions that the surface height follows the Gaussian distribution and the autocovariance function of surface roughness is also Gaussian (see Refs. 1 and 17). Notice that the surface should be slightly rough, so that both rms roughness and autocorrelation length are less than the wavelength of the incidence radiation. When $k$ is neglected and the scattering factors are introduced, the modified Fresnel coefficients between media $j$ and $j'$, $j = 1$, 2, or 3, and $j' = j \pm 1$, are given in the following equations:

$$r_{p,jj'} = \frac{n_j\cos\theta_{j'} - n_{j'}\cos\theta_j}{n_j\cos\theta_{j'} + n_{j'}\cos\theta_j}S_{r,jj'} \tag{3}$$

$$t_{p,jj'} = \frac{2n_j\cos\theta_j}{n_j\cos\theta_{j'} + n_{j'}\cos\theta_j}S_{t,jj'} \tag{4}$$

for $p$ polarization and

$$r_{s,jj'} = \frac{n_j\cos\theta_j - n_{j'}\cos\theta_{j'}}{n_j\cos\theta_j + n_{j'}\cos\theta_{j'}}S_{r,jj'} \tag{5}$$

$$t_{s,jj'} = \frac{2n_j\cos\theta_j}{n_j\cos\theta_j + n_{j'}\cos\theta_{j'}}S_{t,jj'} \tag{6}$$

for $s$ polarization. In the preceding equations, the scattering factors are the same for both polarizations but different for transmission and reflection, namely,[2–6]

$$S_{r,jj'} = \exp\left[-\tfrac{1}{2}(4\pi n_j\sigma\cos\theta_j/\lambda)^2\right] \tag{7}$$

$$S_{t,jj'} = \exp\left\{-\tfrac{1}{2}[2\pi(n_j\cos\theta_j - n_{j'}\cos\theta_{j'})\sigma/\lambda]^2\right\} \tag{8}$$

where $\sigma$ is the rms roughness of the interface.

Note that some relations of the Fresnel coefficients, such as $r_{jj'} = -r_{j'j}$ and $1 + r_{jj'} = t_{jj'}$, do not hold after the modifications because of scattering losses. Furthermore, the energy losses due to surface roughness increase toward shorter wavelengths because of the $\sigma/\lambda$ term in the scattering factors, resulting in a reduction in the fringe contrasts and a decrease in the overall transmittance.[18]

## Spectral Averaging and the Coherence Function

When wave interference in the film is important, the resulting transmittance oscillates periodically as a function of the wave number. The period of oscillation, or the separation between two interference maxima (or minima), is called the free spectral range $\Delta\nu$. For the film shown in Fig. 1, it can be shown that $\Delta\nu = 1/(2n_2 d\cos\theta_2)$ (Ref. 15). The fringe contrast is defined as

$$\Phi = \frac{T_{\max} - T_{\min}}{T_{\max} + T_{\min}} \tag{9}$$

where $T_{\max}$ and $T_{\min}$ are the transmittance maximum and minimum, respectively. In most FT–IR spectrometers, the wave number interval between two consecutive data points is equal to one-half of the resolution specified by the instrument. The actual resolution in the measurement depends on several factors, including the size of the aperture and the divergence of the beam.[19] Aside from the instrument factors, the sample thickness may vary due to nonparallelism or roughness, causing the phase shift $\beta$ to fluctuate and, consequently, reducing the coherence of the incident radiation. Therefore, the fringe contrast in the measured spectrum is less than that

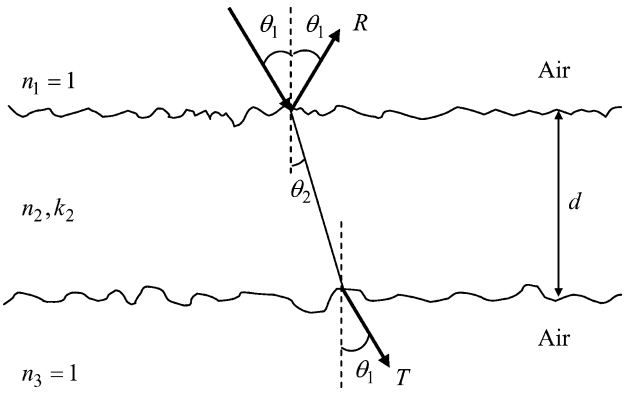


**Fig. 1 Transmittance and reflectance of a thin film with rough surfaces, $\sigma \ll d$ and $k_2 \ll n_2$ assumed.**

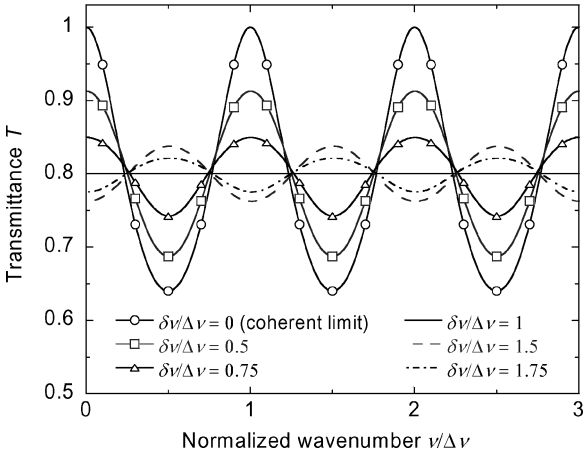


**Fig. 2 Predicated transmittance from the SA method using several coherence spectral widths.**

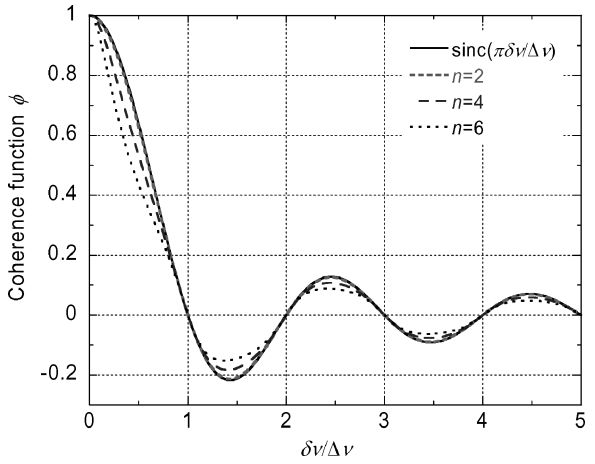


**Fig. 3 Coherence functions vs ratio of coherence spectral width to free spectral range for different refractive indices.**

predicted by wave optics. In contrast, geometric optics completely ignores the interference effects and results in zero fringe contrast. In many practical applications, partial coherence must be taken into consideration to predict the radiative properties in the intermediate regime correctly.

The integral averaging of the transmittance calculated from wave optics over a finite wave number interval yields the same result as the partial coherence formulation.[9–11] The spectral averaging (SA) of the transmittance can be evaluated by

$$\bar{T}(\nu) = \frac{1}{\delta\nu}\int_{\nu-\delta\nu/2}^{\nu+\delta\nu/2} T(\nu')\,\mathrm{d}\nu' \tag{10}$$

where $\nu'$ is a dummy variable and $\delta\nu$, the wave number interval used for the averaging, is called the coherence spectral width in the present work. Figure 2 shows the effect of spectral averaging on the transmittance spectrum for a film with $n=2$ and $k=0$, with various $\delta\nu$ values, at normal incidence. Both the wave number $\nu$ and the coherence spectral width $\delta\nu$ are normalized by the free spectral range $\Delta\nu$, so that the curves are independent of the film thickness. As $\delta\nu/\Delta\nu$ increases from zero (the coherent limit), the fringe contrast decreases until $\delta\nu/\Delta\nu=1$ when all of the fringes disappear. When $\delta\nu/\Delta\nu>1$, however, the fringes reappear, but the peaks and valleys invert from the original. The inversion is the largest when $\delta\nu/\Delta\nu=1.5$. When $\delta\nu/\Delta\nu\gg1$, the fringe contrast becomes negligible, and the transmittance approximates the incoherent limit when geometric optics is applicable.

Although $\delta\nu=0$ and $\delta\nu\to\infty$ correspond to the coherent and incoherent limits, respectively, the magnitude of $\delta\nu$ is not directly related to the degree of coherence in the partial coherence regime. For example, $\delta\nu/\Delta\nu=1.5$ is more coherent than $\delta\nu/\Delta\nu=1$ (when all fringes disappear). The degrees of coherence defined in previous studies[9–11] are difficult to calculate even for smooth films and not applicable to films with rough surfaces. In this paper, a coherence function is introduced as follows:

$$\phi = \frac{\bar{T}(\nu_{\max}) - \bar{T}(\nu_{\min})}{T_{\mathrm{coh}}(\nu_{\max}) - T_{\mathrm{coh}}(\nu_{\min})} \tag{11}$$

where $T_{\mathrm{coh}}$ is the transmittance calculated from the coherence formulation without scattering loss, that is, thin-film optics; $\bar{T}$ is the spectral averaging calculated from Eq. (10) to include partial coherence; and $\nu_{\max}$ and $\nu_{\min}$ are the wave numbers corresponding to transmittance maximum and minimum, respectively, in the coherent limit. In essence, the denominator equals the difference between transmittance extrema in the coherent limit, and the numerator equals the difference in transmittance, when partial coherence is considered, at the same wave numbers.

The coherence function is plotted in Fig. 3 as a function of a dimensionless parameter $\delta\nu/\Delta\nu$ for dielectric thin films with refractive index values equal to 2, 4, and 6 (without absorption). The film thickness is explicitly included in the parameters and does not affect the shape of the curves. The coherence function defined here varies within $(-1, 1)$, and its magnitude quantifies the reduction in the fringe contrast from one in the coherent limit to zero in the incoherent limit. The locations where $\phi=0$ correspond to $\delta\nu=m\Delta\nu$, $m=1, 2, \ldots,$ when all fringes disappear in the transmittance spectra. When $\phi<0$, the peaks and valleys are inverted in the transmittance spectrum, resulting in fringe flipping. The degree of coherence can be approximated as $\mathrm{sinc}(\pi\delta\nu/\Delta\nu)=\sin(\pi\delta\nu/\Delta\nu)/(\pi\delta\nu/\Delta\nu)$ if $|r_{12}r_{23}|<0.25$ (Ref. 10). When $n\le2$, it can be seen from Fig. 3 that the coherence function is approximated by the sinc function. As refractive index increases, however, the coherence function becomes flatter and deviates from the sinc function. Note that if $n>3$ the inequality of $|r_{12}r_{23}|<0.25$ is no longer satisfied, and the degree of coherence defined in Ref. 10 depends not only on the refractive index but also on the film thickness and frequency region, and it is generally not the same as the coherence function defined in Eq. (11). In fact, there exist different expressions for the degree of coherence.[9–11] The coherence function serves the same role as the degree of coherence that helps determine which approach, that is, wave optics, partial coherence formulation, or geometric optics, is most suitable for modeling the radiative properties for a particular case. In addition, Eq. (11) can also be applied to rough surfaces as will be discussed in the next section.

## Results and Discussion

The instrument used to measure the transmittance spectra is the ABB Bomem FTLA2000 series (MB154S) FT–IR spectrometer, with a highest resolution of 1 $\mathrm{cm}^{-1}$. The transmittance spectra were measured at room temperature in the wave number range from 500 to 5000 $\mathrm{cm}^{-1}$ ($2<\lambda<20$ $\mu$m), with a globar source and a pyroelectric detector. A sample holder with an aperture of 6-mm diameter limits the beam diameter on the sample. The sample is placed perpendicularly to the incident beam to measure the transmittance at near normal incidence. The $f$-number of the output beam to the sample is five, yielding a half-cone angle of 6 deg. Therefore, the actual incidence angle is from 0 to 6 deg. The Fresnel coefficients and phase shift do not change significantly if the incidence angle is less than 20 deg. For large incidence angles, however, the nonparallelism between the focal plane and the wafer surface, as well as the polarization, may affect the measurement results. The instrument chamber and sample compartment is purged with $N_2$ gas to reduce the absorption of water vapor and $CO_2$ molecules in the air. The cosine truncation function is used as the apodization function.[19] In most measurements, an average over 16 scans is sufficient to reduce the noise level to below 0.1% in the measured spectra. The uncertainty is estimated to be 0.01 in the transmittance measurements.

The degree of coherence generally decreases toward large wave numbers. Grossman and McDonald[13] used a quadratic relationship

**Table 1 Samples in the present study, film thickness measured using micrometer, topographic data, and fitted thickness and rms roughness**

| Sample number | Material | Surface condition | Thickness, $\mu$m | Topographic data: RMS roughness, $\mu$m | Topographic data: Autocorrelation length, $\mu$m | Least-squares fitting: Thickness, $\mu$m | Least-squares fitting: RMS roughness, $\mu$m |
|---|---|---|---|---|---|---|---|
| 1 | Silicon | DSP | $33.9 \pm 3.9$ | <2 nm | N/A | $35.46 \pm 0.03$ | N/A |
| 2 | CVD diamond | SSP | N/A | 0.32 | 1.1 | $11.4 \pm 0.3$ | $0.35 \pm 0.02$ |
| 3 | Silicon | SSP | $502.9 \pm 5.1$ | $0.40 \pm 0.02$ | $7.5 \pm 3.6$ | $508.4 \pm 1.2$ | $0.57 \pm 0.05$ |
| 4 | Silicon | SSP | $158.3 \pm 1.5$ | $0.68 \pm 0.15$ | $36.3 \pm 0.9$ | $154.0 \pm 0.4$ | N/A |

between the degree of coherence and wave number. In the present study, however, the coherence spectral width $\delta\nu$ is the key parameter needed to perform the spectral averaging. If the change in $n_2$ is neglected, the variation in the phase shift $\beta = 2\pi\nu n_2 d\cos\theta_2$ will be proportional to $\nu$ for a fixed perturbation in $d$. If the coherence spectral width is assumed to be linearly dependent on the phase shift variation, then it should be a linear function of wave number for a given specimen; hence,

$$\delta\nu = a\nu + b \tag{12}$$

The method of least-squares fitting can be used to determine the constants $a$ and $b$ used in Eq. (12), the thickness of the film $d$, and the rms roughness $\sigma$. The standard error of estimate (SEE) between the measured and predicted transmittance is expressed as[20]

$$\text{SEE} = \sqrt{\frac{\sum_{i=1}^{N}[T_m(\nu_i) - T_c(\nu_i; a, b, d, \sigma)]^2}{(N-4)}} \tag{13}$$

where $T_m$ and $T_c$ correspond to the measured and calculated transmittance, respectively, and $N$ is the total number of data points. Notice that $N-4$ is the degree of freedom because four parameters are to be estimated from the least-squares fitting. The best fit is obtained by minimizing the value of SEE in Eq. (13). The uncertainty of the fitted thickness $d$ and rms roughness $\sigma$ are estimated by varying $d$or $\sigma$ from the best-fit value until the SEE is 0.01 greater than the smallest SEE.

Table 1 lists the four samples used in the present study. Sample 1 is a thinned silicon wafer, polished on both sides for the study of the effect of partial coherence independently of surface scattering. Sample 2 is a polycrystalline diamond film. The diamond film was grown by chemical vapor deposition on a smooth substrate; then the middle portion of the substrate was etched away, leaving a diamond film in the middle supported by a ring of the remaining substrate. The surface originally attached to the substrate is quite smooth, and the other surface is rough. The size of the diamond film is about 15 mm in diameter and the outer diameter of the supporting ring is approximately 25 mm. Samples 3 and 4 are two SSP silicon wafers of different thickness and surface conditions. All of the silicon wafers (including sample 1) are single crystalline with $\langle 100\rangle$ orientation and lightly doped. The silicon specimens are cut from large wafers to a size of approximately $12 \times 12$ mm$^2$. A micrometer was used to measure the film thickness of the silicon specimens only because the diamond film is too fragile. The average and standard deviation of the thickness are listed in Table 1. The topographic data for the silicon wafer were obtained from the stylus profilometer measurements, whereas an AFM provided the topographic information of the diamond film.

Figure 4 shows the measured and predicted transmittance for the thin DSP silicon, sample 1. The transmittance in the incoherent limit using geometric optics is plotted in Fig. 4a for comparison, whereas Figs. 4b and 4c zoom in the spectrum to a narrow spectral region and show a comparison of the measurement with that predicted with or without spectral averaging. The measurement was conducted with a resolution of 1 cm$^{-1}$ to achieve the highest possible coherence with the instrument. In the calculation, the tabulated data for the optical constants of silicon are used.[21] The free spectral range $\Delta\nu$ of this specimen is approximately 41.3 cm$^{-1}$, which varies slightly due to the dispersion of silicon in the wave number region of 500 to 5000 cm$^{-1}$. From the least-squares fitting, the thickness of the silicon wafer is determined to be $35.46 \pm 0.03$ $\mu$m, which agrees well with the value measured by a micrometer: $33.9 \pm 3.9$ $\mu$m. The coherence spectral width determined by the least-squares fitting is $\delta\nu = 0.0061\nu + 4.3$ cm$^{-1}$, which varies from 7 to 35 cm$^{-1}$ in the measured spectral region. Without spectral averaging, the coherence formulation overpredicts the fringe contrasts, especially at shorter wavelengths, as shown in Fig. 4c. The SEE between the measured and calculated transmittance is 0.039 with spectral averaging (SA) and 0.138 without SA. A closer look at the coherence spectral width provides an idea about the effect of partial coherence. For instance, at $\nu = 1000$ cm$^{-1}$ the coherence spectral width is $\delta\nu = 10.4$ cm$^{-1}$, which is much larger than the resolution of the instrument, suggesting that the nonparallelism of the sample surfaces may be the dominating factor that reduces the fringe contrast in the measured transmittance, especially at short wavelengths.

Figure 5 shows the transmittance of sample 2, which has a large free spectral range $\Delta\nu \approx 200$ cm$^{-1}$ because the film is very thin (11.4 $\mu$m), and the refractive index of diamond is smaller than that of silicon. The resolution used in the measurement is 4 cm$^{-1}$. The reduction of transmittance, as well as fringe contrasts toward shorter wavelengths (large wave numbers) can be clearly seen. In modeling the transmittance of the diamond specimen, adjusting the refractive index is needed to reduce the offset between the measured and predicted spectra. This is because the tabulated values[22] are for single-crystal diamond, whereas the CVD diamond film consists of polycrystalline structures, formed when grown on nondiamond substrates.[6] Petrich and Stenzel[14] also noted similar deviations in their determination of the optical constants of CVD diamond film and attributed the effect to the polycrystalline structure of the material. In the present study, it was found that a constant value of 2.2 can be used for the refractive index of the diamond film to obtain good fitting. This value is slightly less than that for single crystal, which is near 2.4 (Ref. 22).

It can be seen from Fig. 5 that SST alone predicts much larger fringe contrasts, particularly in the shorter wave number region, as compared with the experiments. When SA is applied, the predicted transmittance agrees well with the measured data. Note in Fig. 5b that the fringe contrast first decreases as the wave number increases until $\nu \approx 1700$ cm$^{-1}$, where the fringe disappears and reappears at $\nu > 1700$ cm$^{-1}$ with the maximum and minimum inverted. As explained in the preceding section, this fringe disappearing should occur at $\delta\nu = \Delta\nu$, and when $\delta\nu > \Delta\nu$, the peaks and valleys of the fringes interchange from the original positions, resulting in fringe flipping, as shown in Fig. 5b. The predicted transmittance with SA describes well the fringe disappearing and fringe flipping. The coherence spectral width from the least-squares fitting is estimated as $\delta\nu = 0.127\nu - 13.0$ cm$^{-1}$ for $500 < \nu < 3000$ cm$^{-1}$. Note that $\delta\nu$ is equal to $\Delta\nu$ at $\nu \approx 1700$ cm$^{-1}$, and spectral averaging is only applied to wave numbers less than 3000 cm$^{-1}$ because all fringes disappear beyond 3000 cm$^{-1}$ due to the reduction of coherence by scattering. The small dips near 2900 cm$^{-1}$ in the measured spectra can be explained by the residual water vapor absorption. From the least-squares fitting, the thickness is estimated to be $11.4 \pm 0.3$ $\mu$m, and the rms roughness of surface is $0.35 \pm 0.02$ $\mu$m. The rms roughness measured by the AFM is 0.32 $\mu$m, less than 10% difference from the fitted value. The SEE is calculated to be 0.007 with spectral averaging and 0.021 without it.

Figure 6 shows the transmittance of sample 3, an SSP silicon about 500 $\mu$m thick. The free spectral range $\Delta\nu$ is approximately 2.9 cm$^{-1}$, and the instrument resolution is set to 1 cm$^{-1}$ in the

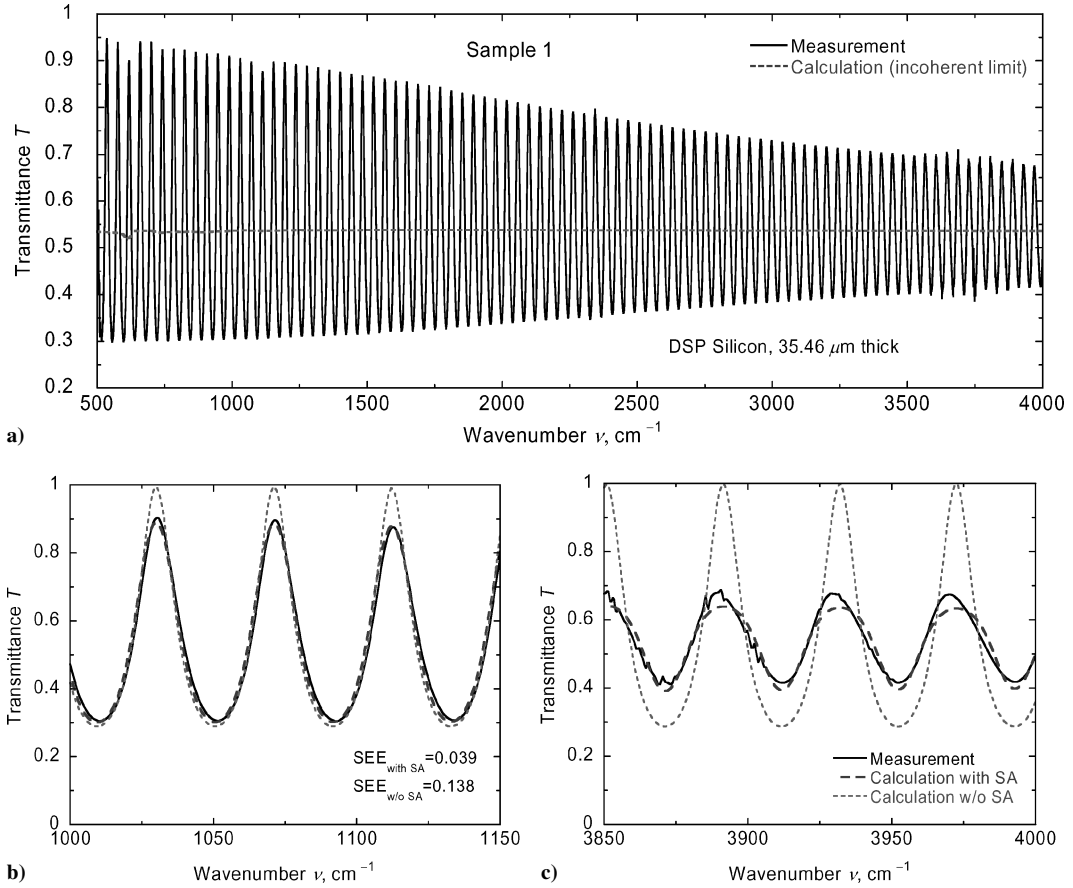


**Fig. 4 Spectral transmittance of sample 1, DSP silicon: a) from 500 to 4000 cm$^{-1}$, b) zoomed from 1000 to 1150 cm$^{-1}$, and c) zoomed from 3850 to 4000 cm$^{-1}$.**

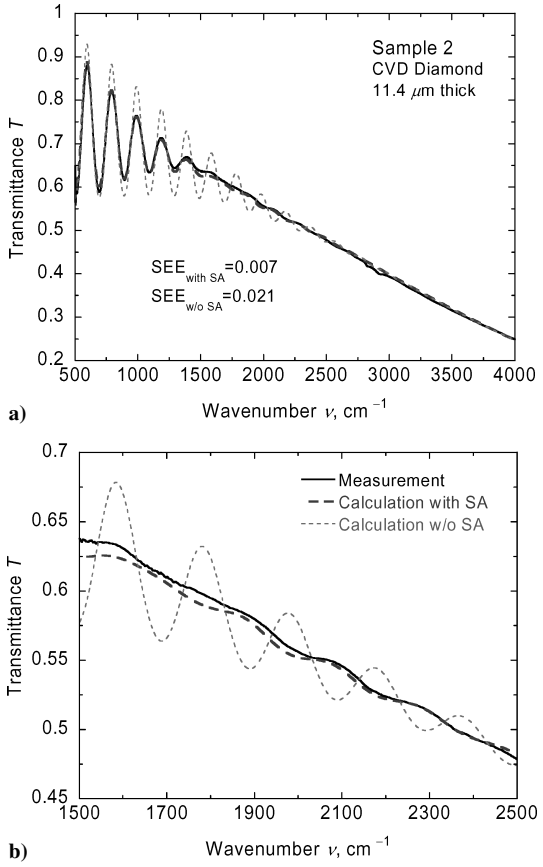


**Fig. 5 Spectral transmittance of sample 2, CVD diamond: a) from 500 to 4000 cm$^{-1}$, and b) zoomed from 1500 to 2500 cm$^{-1}$.**

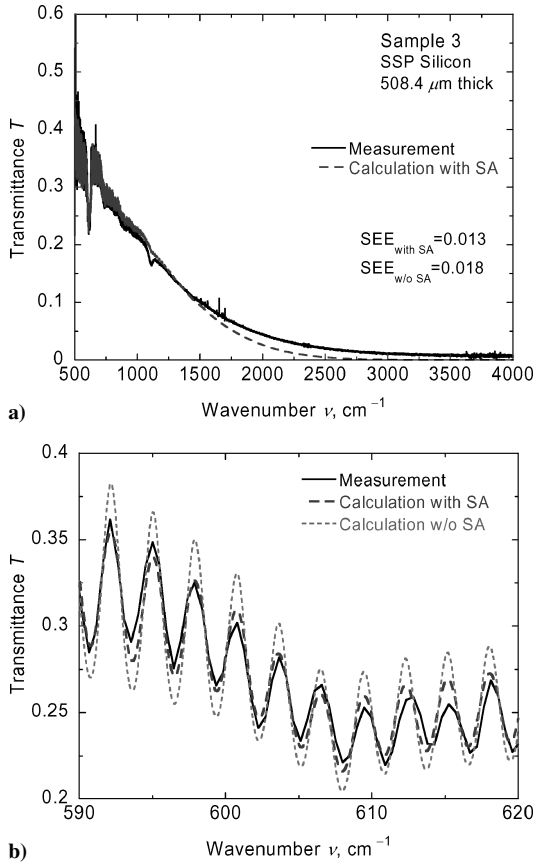


**Fig. 6 Spectral transmittance of the sample 3, SSP silicon: a) from 500 to 4000 cm$^{-1}$ and b) zoomed from 590 to 620 cm$^{-1}$.**

measurement. The fringe contrasts are much smaller compared with those for the earlier samples. Optical phonon absorption is noticeable near 615 and 1100 $cm^{-1}$, resulting in some absorption in silicon that can be clearly seen from the spectrum. Even in this absorbing region, the $k$ of silicon is less than 0.0013. Thus, the slightly absorbing assumption is still valid. Because the effect of absorption is included in the internal transmissivity, the formulation can correctly predict the transmittance in the absorbing region, including the reduction of fringe contrast caused by absorption. Furthermore, the residual water vapor caused some fluctuations around 1600, 2400, and 3700 $cm^{-1}$. From the fitting, the thickness of the sample is determined to be $508.4 \pm 1.2$ $\mu$m, comparable with that measured using a micrometer of $502.9 \pm 5.1$ $\mu$m. The zoomed plot in Fig. 6b shows that using SA results in a slightly improved agreement with the measured spectrum at smaller wave numbers. Beyond 1000 $cm^{-1}$, however, all fringes disappear, and SA is not necessary. At wave numbers greater than 1300 $cm^{-1}$, the predicted transmittance is consistently lower than the measured one. From Table 1, note that the autocorrelation length of this sample is $7.5 \pm 3.6$ $\mu$m, which is about the same as the wavelength of the incident radiation at 1300 $cm^{-1}$. If the wavelength of the incident radiation is shorter than the size of irregularities of rough surface, the scattering from rough surfaces may not be well described by the scalar scattering theory. For this reason, the least-squares fitting is performed for wave numbers less than 1300 $cm^{-1}$. Because of the narrow spectral region, the coherence spectral width is taken as a constant equal to 2.1 $cm^{-1}$. The rms roughness of the rough surface is estimated to be $0.57 \pm 0.05$ $\mu$m. The rms roughness of this specimen measured with a profilometer is $0.40 \pm 0.02$ $\mu$m, which is 45% less than the fitted value. The SEE between measured and calculated transmittance is 0.013 with SA and 0.018 without SA. Applying SA does not significantly improve the fitting result for this sample because the fringe contrasts have been largely reduced by the surface roughness.

The transmittance for sample 4, another SSP silicon with a thickness near 150 $\mu$m, is shown in Fig. 7a together with the calculated spectra with different rms roughness values. The fringes in the computed spectra are intentionally reduced using SA to illustrate clearly the differences between the spectra. Note that SST fails to predict the transmittance for this specimen, no matter what $\sigma$ is used. Surface roughness generally leads to a decrease in the transmittance at higher wave number according to the scattering factors. However, the measured result shows little decrease in transmittance beyond 1000 $cm^{-1}$. When the fringe locations are matched at small wave numbers, the thickness of the sample is estimated as $154.0 \pm 0.4$ $\mu$m, which is close to that measured with a micrometer. The reason for the failure of SST is believed to be due to the large correlation length as shown in Table 1. The rough surface obtained from an optical microscope is shown in Fig. 7b, and it reveals large lateral features even though the measured rms roughness is on the same order as that of sample 3. Figure 7b clearly shows that the grain boundaries of the polysilicon over layer. The size of the grain boundary ranges from 10 to 40 $\mu$m, although the height difference between peaks and valleys is only 1 to 2 $\mu$m. The autocorrelation length of this sample is estimated to be $36.3 \pm 0.9$ $\mu$m from the surface profilometer data. Because SST is based on wave optics for the case when the wavelength of the incident radiation is larger than the size of the irregularities of rough surfaces, it is not applicable to a surface with large microstructures.[1,23] In contrast, geometric optics may be more appropriate in the prediction of scattering from the rough surface that has a large autocorrelation length, even though the rms roughness is smaller than the wavelength. Note that wavelength independence is a hallmark of the geometric optics formulation based on incoherent scattering. The slope distribution is an important factor in the geometric optics approximation to model the light scattering from rough surfaces.[24] A detailed study using geometric optics to account for the scattering loss, however, is beyond the scope of the current work.

Even though SST is based on the coherence formulation, the fringe contrasts significantly decrease once the surface is rough. Hence, the coherence function for rough surfaces should be less than one even without SA. Caution must be taken to calculate the coherence function for samples with rough surfaces. The denominator of

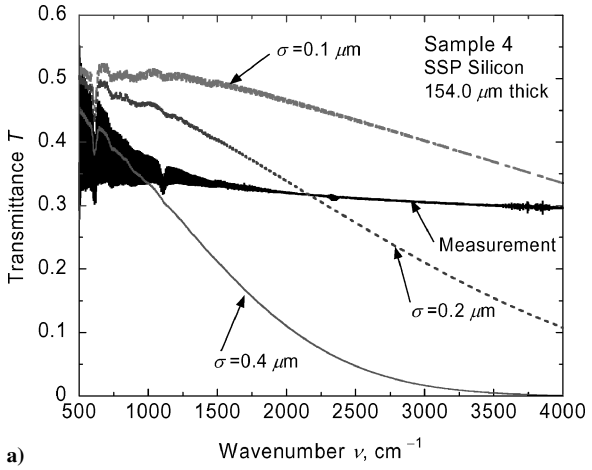


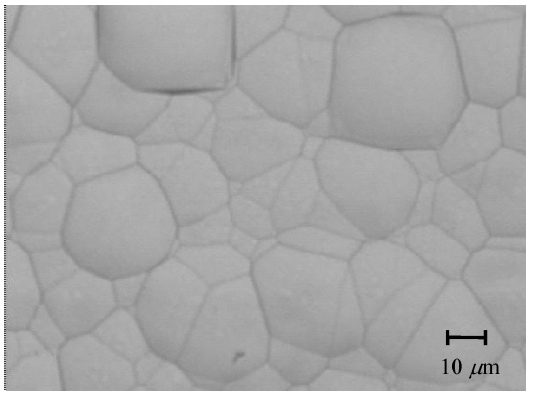


**Fig. 7 Transmittance and surface image of sample 4, SSP silicon with a polysilicon overlayer: a) measured and calculated transmittance spectra; b) surface image of the grain boundaries on the polysilicon surface.**

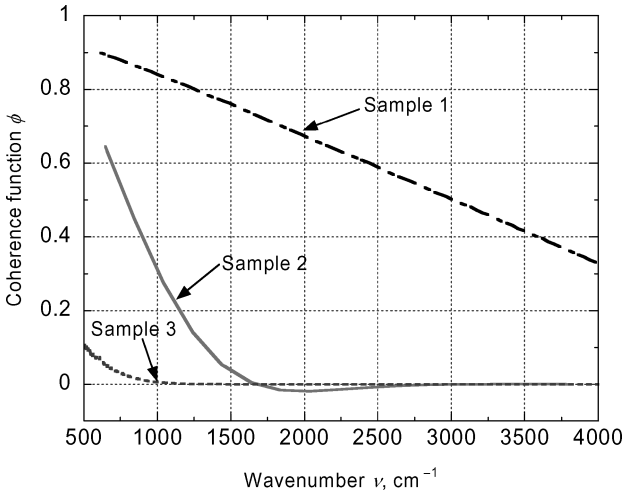


**Fig. 8 Coherence functions vs wave number for samples 1, 2, and 3.**

Eq. (11) should be calculated using the coherence transmittance for smooth surfaces to give the largest difference. When the numerator of Eq. (11) is calculated, modification of the transmittance spectrum is necessary because the transmittance decreases as the wave number increases due to scattering losses. Consequently, even though no fringes exist after the SA, the numerator is not equal to zero because the spectrally averaged transmittance is not the same at $\nu_{max}$ and $\nu_{min}$. The transmittance in the incoherent limit is subtracted from spectrally averaged transmittance to level the transmittance spectrum. Notice that a measured spectrum can also be used to calculate the numerator of Eq. (11) instead of the calculated transmittance with SA.

The coherence functions vs wave number for samples 1–3 are plotted in Fig. 8. It is clear that the DSP sample is much more coherent than the rough ones. Because the fringes in the transmittance of the samples 2 and 3 disappear at large wave numbers, the coherence functions also become zero, indicating that transmittance is completely incoherent at short wavelengths of the measured spectral region. For sample 2, locations where fringes are flipped can be clearly seen from the negative values of the coherence function at wave numbers from 1700 to 2500 $cm^{-1}$. It is obvious that sample 2 is more coherent than sample 3. Notice from Eqs. (7) and (8) that the scattering factor depends on both the refractive index and rms roughness. Because the refractive index ($n = 3.43$) and rms roughness ($\sigma = 0.57$ $\mu$m) of sample 3 are both larger than those of sample 2 ($n = 2.2$, $\sigma = 0.35$ $\mu$m), the scattering factors are much smaller for sample 3 than for sample 2, resulting in a greater reduction in the transmittance and coherence. This explains why sample 3 is less coherent than sample 2, even though sample 3 has a much smaller $\delta\nu$ than sample 2.

## Conclusions

The effect of surface roughness on the spectral transmittance of thin films is investigated using SST combined with the SA method. Two noticeable features, that is, fringe disappearing and fringe flipping, in the measured transmittance spectrum of a diamond film can be accurately predicted. This study clearly demonstrates that partial coherence is a crucial factor in modeling the transmittance of thin films with rough surfaces when partial coherence is important. In the wave number range from 500 to 5000 $cm^{-1}$, the coherence spectral width is generally wave number dependent and is postulated as a linear function of the wave number. In addition, a coherence function is recommended as a measure of the degree of coherence and can be extended to rough surfaces. Note that SST has its limitations and is not applicable for samples that have a large autocorrelation length compared to the wavelength of the incident radiation. When this is the case, geometric optics may be an alternative approach to evaluate the effect of roughness on the transmittance.

## Acknowledgments

This work was supported by the National Science Foundation (CTS-0236831), the National Institute of Standards and Technology, and the Georgia Institute of Technology Focused Research Program. The authors thank J. Robert Mahan for his valuable comments and Yu-Bin Chen and Qunzhi Zhu for their help with the surface characterization.

## References

[1]Beckmann, P., and Spizzichino, A., *The Scattering of Electromagnetic Waves from Rough Surfaces*, Artech House, Norwood, MA, 1987, Chap. 5.

[2]Filinski, I., "The Effects of Sample Imperfections on Optical Spectra," *Physica Status Solidi B*, Vol. 49, No. 2, 1972, pp. 577–588.

[3]Carniglia, C. K., "Scalar Scattering Theory for Multilayer Optical Coatings," *Optical Engineering*, Vol. 18, No. 2, 1979, pp. 104–115.

[4]Mitsas, C. L., and Siapkas, D. I., "Generalized Matrix Method for Analysis of Coherent and Incoherent Reflectance and Transmittance of Multilayer Structures with Rough Surfaces, Interfaces, and Finite Substrates," *Applied Optics*, Vol. 34, No. 10, 1995, pp. 1678–1683.

[5]Ohlidal, I., Navratil, K., and Ohlidal, M., "Scattering of Light from Multilayer Systems with Rough Boundaries," *Progress in Optics*, Vol. 34, 1995, pp. 249–331.

[6]Robins, L. H., Farabaugh, E. N., and Feldman, A., "Determination of the Optical Constants of Thin Chemical-Vapor-Deposited Diamond Window from 0.5 to 6.5 eV," *Proceedings of SPIE*, Vol. 1534, July 1991, pp. 105–116.

[7]Poruba, A., Fejfar, A., Remes, Z., Springer, J., Vanecek, M., Kocka, J., Meier, J., Torres, P., and Shah, A., "Optical Absorption and Light Scattering in Microcrystalline Silicon Thin Films and Solar Cells," *Journal of Applied Physics*, Vol. 88, No. 1, 2000, pp. 148–160.

[8]Wong, P. Y., Trefethen, L. M., and Miaoulis, L. N., "Cross Correlation of Optical Properties of Thin Films Under Thermal Radiation," *Journal of Applied Physics*, Vol. 72, No. 10, 1992, pp. 4884–4887.

[9]Chen, G., and Tien, C. L., "Partial Coherence Theory of Thin Film Radiative Properties," *Journal of Heat Transfer*, Vol. 114, No. 3, 1992, pp. 636–643.

[10]Richter, K., Chen, G., and Tien, C. L., "Partial Coherence Theory of Multilayer Thin-Film Optical Properties," *Optical Engineering*, Vol. 32, No. 8, 1993, pp. 1897–1903.

[11]Zhang, Z. M., "Optical Properties of Layered Structures for Partially Coherent Radiation," *Proceedings of the 10th International Heat Transfer Conference*, edited by G. F. Hewitt, IChemE, Brighton, U.K., Vol. 2, 1994, pp. 177–182.

[12]Anderson, C. F., and Bayazitoglu, Y., "Radiative Properties of Films Using Partial Coherence Theory," *Journal of Thermophysics and Heat Transfer*, Vol. 10, No. 1, 1996, pp. 26–32.

[13]Grossman, E. N., and McDonald, D. G., "Partially Coherent Transmittance of Dielectric Lamellae," *Optical Engineering*, Vol. 34, No. 5, 1995, pp. 1289–1295.

[14]Petrich, R., and Stenzel, O., "Modeling of Transmittance, Reflectance and Scattering of Rough Polycrystalline CVD Diamond Layers in Application to the Determination of Optical Constants," *Optical Materials*, Vol. 3, No. 1, 1994, pp. 65–76.

[15]Zhang, Z. M., Fu, C. J., and Zhu, Q. Z., "Optical and Thermal Radiative Properties of Semiconductors Related to Micro/Nanotechnology," *Advances in Heat Transfer*, Vol. 37, 2003, pp. 179–296.

[16]Zhang, Z. M., "Optical Properties of a Slightly Absorbing Film for Oblique Incidence," *Applied Optics*, Vol. 38, No. 1, 1999, pp. 205–207.

[17]Davies, H., "The Reflection of Electromagnetic Waves from a Rough Surface," *Proceedings of the Institution of Electrical Engineers*, Vol. 101, Pt. 4, No. 6, 1954, pp. 209–214.

[18]Montecchi, M., Montereali, R. M., and Nichelatti, E., "Reflectance and Transmittance of a Slightly Inhomogeneous Thin Film Bounded by Rough, Unparallel Interfaces," *Thin Solid Films*, Vol. 396, Nos. 1–2, 2001, pp. 262–273.

[19]Griffiths, P. R., and de Haseth, J. A., *Fourier Transform Infrared Spectrometry*, Wiley, New York, 1986, Chap. 1.

[20]Lipson, C., and Sheth, N. J., *Statistical Design and Analysis of Engineering Experiments*, McGraw–Hill, New York, 1973, Chap. 13.

[21]Edwards, D. F., "Silicon (Si)," *Handbook of Optical Constants of Solids*, edited by E.D. Palik, Academic Press, Orlando, FL, 1985, pp. 547–569.

[22]Edwards, D. F., and Philipp, H. R., "Cubic Carbon (Diamond)," *Handbook of Optical Constants of Solids*, edited by E. D. Palik, Academic Press, Orlando, FL, 1985, pp. 665–673.

[23]Bennett, H. E., and Porteus, J. O., "Relation Between Surface Roughness and Specular Reflectance at Normal Incidence," *Journal of the Optical Society of America*, Vol. 51, No. 2, 1961, pp. 123–129.

[24]Tang, K., Dimenna, R. A., and Buckius, R. O., "Regions of Validity of the Geometric Optics Approximation for Angular Scattering from Very Rough Surfaces," *International Journal of Heat and Mass Transfer*, Vol. 40, No. 1, 1997, pp. 49–59.